



Winter Internship Project

Report

Karmukilan Somasundaram

National Institute of Science Education and Research
Tehsildar Office, Khurda
Pipli, Near, Jatni, Odisha 752050

Under the guidance of

Dr.V K Chandrasekar

Associate professor
School of Electrical and Electronics Engineering
SASTRA deemed University
Trichy-Tanjore Road, Thirumalaisamudram
Thanjavur, Tamilnadu

January 10, 2025

Acknowledgments

I would like to express my gratitude towards Dr.V K Chandrasekar for providing me with the opportunity to work under his commendable guidance. I would also like to thank Dr. Manoranjani for her guidance and support. I am grateful for National Institute of Science Education and Research for granting me this opportunity.

Abstract

main goals of this report would be to familiarize ourselves with the Kuramoto model. The study will be restricted to the mean field model . The system under the continuum limit will be obtained and certain branches of solutions and their bifurcations will be investigated. We will also analyze the bifurcation diagram for the 2 and 3 oscillators system. Finally, findings from the previous proceedings will be verified by numerical simulations.

Contents

1	Introduction	4
2	Continuum limit of the Kuramoto model	5
2.1	Stationary solutions	5
3	2 oscillator system and special cases of 3 oscillator system	9
3.1	2 oscillator system	9
3.2	3 oscillator system	10
4	Numerical Simulations	14
4.1	R vs t	15
4.2	R vs K	17
5	Conclusion	19

1 Introduction

Synchronization is an interesting phenomena observed in biological systems, physical systems and even social dynamic models. Synchronization demonstrates the mutual co-operation of individuals which can be observed in nature. One such well studied model is the Kuramoto model. Despite the significant interest in the field there still remains open problems suggestive of the intricate and complex nature of the system.

For finite number of oscillators the system is as follows:

$$\begin{aligned}\dot{\theta}_1 &= \omega_1 + \frac{K}{N} \sum_{j=2}^N \sin(\theta_j - \theta_1) \\ &\vdots \\ \dot{\theta}_i &= \omega_i + \frac{K}{N} \sum_{j=1, j \neq i}^N \sin(\theta_j - \theta_i) \\ &\vdots \\ \dot{\theta}_N &= \omega_N + \frac{K}{N} \sum_{j=1}^{N-1} \sin(\theta_j - \theta_N)\end{aligned}$$

this is the Kuramoto model with mean field coupling (equally weighted interactions) in general the velocity will be

$$\dot{\theta}_i = \omega_i + \sum_{j=1, j \neq i}^N K_{ij} \sin(\theta_j - \theta_i) \quad (1)$$

Geometrically the system can be visualized as N oscillators in an unit circle where the angle from the X-axis will be the phase and the natural frequencies can be distributed with a function $g(\omega)$. From the reference frame rotating with angular velocity equal to the first moment of $g(\omega)$ the natural frequency distribution would have a zero mean, this implies studying the latter system is necessary and sufficient.

In order to study synchronization and write the system in a more compact form it's convenient to define a complex order parameter [1]

$$r e^{i\psi} = \frac{1}{N} \sum_{j=1}^N e^{i\theta_j} \quad (2)$$

It is evident that for all time

$$0 \leq r(t) \leq 1$$

this allows us to write

$$\dot{\theta}_i = \omega_i + K r \sin(\psi - \theta_i) \quad (3)$$

For the mean field coupling the order parameter's time evolution can be used to study synchronization of the system. It is to be noted that this idea is feasible only due to the structure of coupling in the system. For example, systems which have close range coupling allows a possibility that fractions of oscillators can bunch up and rotate in a fashion which leaves the order parameter close to zero [1]. This counter example also illustrates the symmetry of the mean field model.

2 Continuum limit of the Kuramoto model

When the number of oscillators approach infinity, we can approximate the distributions to be continuous and analyze their densities [2]. For each ω , $\rho(\theta, \omega, t)d\theta$ denote the probability density of oscillators with natural frequency ω between θ and $\theta + d\theta$. The natural progression would be to normalize this non-negative, periodic function in θ as

$$\int_{-\pi}^{\pi} \rho(\theta, \omega, t) d\theta = 1 \quad (4)$$

Time evolution of ρ will be governed by the continuity equation

$$\frac{\partial \rho}{\partial t} = -\frac{\partial(\rho v)}{\partial \theta} \quad (5)$$

where $v(\theta, \omega, t) = \omega + K r \sin(\psi - \theta)$. The continuity equation basically emphasizes that oscillators with natural frequency ω remains conserved. In this setting we define the order parameter $r(t)$ and $\psi(t)$ as

$$r e^{i\psi} = \int_{-\pi}^{\pi} \int_{-\infty}^{\infty} e^{i\theta} \rho(\theta, \omega, t) g(\omega) d\omega d\theta \quad (6)$$

Now, the equations (4), (5), (6) have to be solved together for $\rho(\theta, \omega, t)$.

2.1 Stationary solutions

We will try to solve the system for the stationary case where $\frac{\partial \rho}{\partial t} = 0$. The trivial solution obeying the normalization constraint will be $\rho = \frac{1}{2\pi}$. This corresponds to the incoherent state of the system and this remains a solution for all values of coupling

K with the stability of the solution depending on K. Now in-order to find a simple non-trivial solution for the system we induce a splitting of the oscillators based on their natural frequency ω which will prove useful when we analyze the continuity equation. For the group of oscillators with $|\omega| \leq Kr$ and appropriate θ value the angular velocity at that θ and ω will be zero which satisfies the continuity equation for $|\omega| \leq Kr$. So if for every such omega all the density is concentrated in these angles there will be no time evolution of these distributions, this fact with the normalization constraint naturally calls for the dirac delta distributions. Now, for the remaining ω values we can arrive at the equation directly from the continuity equation. So, the solution $\rho(\theta, \omega, t)$ will be

$$\rho(\theta, \omega, t) = \begin{cases} \delta(\theta - \psi - \sin^{-1}(\frac{\omega}{Kr})) & \text{if } |\omega| \leq Kr, \\ \frac{C}{|\omega - Kr \sin(\psi - \theta)|} & \text{elsewhere} \end{cases} \quad (7)$$

To determine the constant C in eq(7) we can use the normalization constraint which yields

$$C = \frac{\sqrt{(\omega)^2 - (Kr)^2}}{2\pi} \quad (8)$$

With the solution obtained we will try to calculate the order parameter of this partially synchronized state of the system. from eq (6)

$$\begin{aligned} re^{i\psi} &= \int_{-\pi}^{\pi} \int_{-\infty}^{\infty} e^{i\theta} \rho(\theta, \omega, t) g(\omega) d\omega d\theta \\ \Rightarrow re^{i\psi} &= \int_{-\pi}^{\pi} \int_{|\omega| \leq Kr} e^{i\theta} \rho(\theta, \omega, t) g(\omega) d\omega d\theta \\ &\quad + \int_{-\pi}^{\pi} \int_{|\omega| > Kr} e^{i\theta} \rho(\theta, \omega, t) g(\omega) d\omega d\theta \\ \Rightarrow re^{i\psi} &= \int_{-\pi}^{\pi} \int_{|\omega| \leq Kr} e^{i\theta} \delta\left(\theta - \psi - \sin^{-1}\left(\frac{\omega}{Kr}\right)\right) g(\omega) d\omega d\theta \\ &\quad + \int_{-\pi}^{\pi} \int_{|\omega| > Kr} e^{i\theta} \frac{C}{|\omega - Kr \sin(\psi - \theta)|} g(\omega) d\omega d\theta \\ \Rightarrow r &= \int_{-\pi}^{\pi} \int_{|\omega| \leq Kr} e^{i(\theta - \psi)} \delta\left(\theta - \psi - \sin^{-1}\left(\frac{\omega}{Kr}\right)\right) g(\omega) d\omega d\theta \\ &\quad + \int_{-\pi}^{\pi} \int_{|\omega| > Kr} e^{i(\theta - \psi)} \frac{C}{|\omega - Kr \sin(\psi - \theta)|} g(\omega) d\omega d\theta \end{aligned} \quad (9)$$

If $g(\omega) = g(-\omega)$, then $\rho(\theta + \pi, -\omega) = \rho(\theta, \omega)$ implies that the second integral will be zero which simplifies equation (9)

$$\begin{aligned}
r &= \int_{-Kr}^{+Kr} \int_{-\pi}^{\pi} e^{i(\theta-\psi)} \delta(\theta - \psi - \sin^{-1}(\frac{\omega}{Kr})) g(\omega) d\theta d\omega \\
\Rightarrow r &= \int_{-Kr}^{Kr} e^{i \sin^{-1}(\frac{\omega}{Kr})} g(\omega) d\omega \\
\Rightarrow r &= \int_{-Kr}^{Kr} \cos(\sin^{-1}(\frac{\omega}{Kr})) g(\omega) d\omega + \int_{-Kr}^{Kr} \frac{\omega g(\omega)}{Kr} d\omega \\
\Rightarrow r &= \int_{-Kr}^{Kr} \cos(\sin^{-1}(\frac{\omega}{Kr})) g(\omega) d\omega
\end{aligned}$$

by a change of variable $\omega = Kr \sin(\theta)$ we get,

$$\begin{aligned}
r &= \int_{-\frac{\pi}{2}}^{\frac{\pi}{2}} \cos(\theta) g(Kr \sin(\theta)) Kr \cos(\theta) d\theta \\
r &= Kr \int_{-\frac{\pi}{2}}^{\frac{\pi}{2}} \cos^2(\theta) g(Kr \sin(\theta)) d\theta
\end{aligned} \tag{10}$$

Equation (10) always has the trivial solution of $\rho = \frac{1}{2\pi}$ corresponding to incoherence. For $r \neq 0$ we have a solution corresponding to the partially synchronized state which satisfies

$$1 = K \int_{-\frac{\pi}{2}}^{\frac{\pi}{2}} \cos^2(\theta) g(Kr \sin(\theta)) d\theta \tag{11}$$

This state bifurcates continuously from the incoherent phase around a critical coupling K_c . K_c can be determined from eq (11)

$$\begin{aligned}
\frac{1}{K_c} &= \lim_{r \rightarrow 0^+} \int_{-\frac{\pi}{2}}^{\frac{\pi}{2}} \cos^2(\theta) g(Kr \sin(\theta)) d\theta \\
\Rightarrow \frac{1}{K_c} &= \int_{-\frac{\pi}{2}}^{\frac{\pi}{2}} \cos^2(\theta) g(\lim_{r \rightarrow 0^+} Kr \sin(\theta)) d\theta \\
\Rightarrow \frac{1}{K_c} &= \int_{-\frac{\pi}{2}}^{\frac{\pi}{2}} \cos^2(\theta) g(0) d\theta \\
\Rightarrow \frac{1}{K_c} &= \frac{\pi g(0)}{2} \\
\Rightarrow K_c &= \frac{2}{\pi g(0)}
\end{aligned}$$

For a distribution $g(\omega)$, g can be expanded in powers of Kr around the bifurcation point.

$$1 \approx K \int_{-\frac{\pi}{2}}^{\frac{\pi}{2}} \cos^2(\theta) [g(0) + g'(0)Kr \sin(\theta) + g''(0)\frac{K^2 r^2 \sin^2 \theta}{2}] d\theta \quad (12)$$

By construction $g'(0) = 0$. so we have

$$\begin{aligned} 1 &\approx K \int_{-\frac{\pi}{2}}^{\frac{\pi}{2}} \cos^2(\theta) g(0) d\theta + \frac{K}{2} \int_{-\frac{\pi}{2}}^{\frac{\pi}{2}} \cos^2(\theta) g''(0) K^2 r^2 \sin^2(\theta) d\theta \\ \implies 1 &\approx \frac{K}{K_c} + \frac{1}{2} K^3 r^2 \int_{-\frac{\pi}{2}}^{\frac{\pi}{2}} \cos^2(\theta) \sin^2(\theta) g''(0) d\theta \\ \implies 1 &\approx \frac{K}{K_c} + K_c^2 K r^2 g''(0) \frac{\pi}{16} \\ \implies r &\approx \sqrt{\frac{16}{\pi K_c^2 K}} \sqrt{\frac{\mu}{-g''(0)}} \end{aligned}$$

where $\mu = \frac{K-K_c}{K_c}$ since this expansion is around the onset of synchronization, the order parameter obeys the square root scaling given by

$$r \approx \sqrt{\frac{16}{\pi K_c^3}} \sqrt{\frac{\mu}{-g''(0)}} \quad (13)$$

Sometimes ' \sim ' relation is also used which compares two functions in the limit as $\epsilon \rightarrow 0$

$$f(\epsilon) \sim g(\epsilon) \iff \lim_{\epsilon \rightarrow 0} \frac{f(\epsilon)}{g(\epsilon)} = 1$$

for a special distribution of the natural frequency given by

$$g(\omega) = \frac{\frac{\gamma}{\pi}}{\gamma^2 + \omega^2}$$

the order parameter can be found directly by substituting for g in eq (10) which results in an exact relation for all $K_c \leq K$

$$r = \sqrt{1 - \frac{K_c}{K}} \quad (14)$$

3 2 oscillator system and special cases of 3 oscillator system

In order to better understand the underlying structure of the Kuramoto model and the relation between synchronization and the coupling it is natural to start with the finite and simple cases like $N=2,3$. We will solve the system for fixed points ,investigate the nature of flow around these points and understand the bifurcation as coupling constant K is varied.

3.1 2 oscillator system

The analysis of the Kuramoto model under the continuum limit model might have been a bit complicated. In order to appreciate the structure of the particular finite system of oscillators we must start studying the simplest case of 2 oscillator system

$$\begin{aligned}\dot{\theta}_1 &= \omega_1 + \frac{K}{2} \sin(\theta_2 - \theta_1) \\ \dot{\theta}_2 &= \omega_2 + \frac{K}{2} \sin(\theta_1 - \theta_2)\end{aligned}\tag{15}$$

Here we subtract both the equations to arrive at

$$\dot{\phi} = \Omega - K \sin(\phi)\tag{16}$$

where $\phi = \theta_2 - \theta_1$ and $\Omega = \omega_2 - \omega_1$,observe that the fixed points in eq (16) corresponds to the synchronized state of the system. This naturally eliminates fixed points for $K < \Omega$. Whenever $\Omega \leq K$ we get $\phi = \sin^{-1}(\frac{\Omega}{K})$ is a fixed point which implies the system is synchronized whenever the phase difference is $\sin^{-1}(\frac{\Omega}{K})$. Both stable and unstable fixed points can be observed for different phase difference ϕ ; For the special case when $K = \Omega$ semi stable fixed points are also observed. In order to understand the bifurcation as parameter K is varied we define the average oscillator frequency $\bar{\Omega}$

$$\begin{aligned}T &= \int_{-\pi}^{\pi} \frac{d\phi}{\Omega - K \sin(\phi)} = \frac{2\pi}{\sqrt{\Omega^2 - K^2}} \\ \bar{\Omega} &= \frac{2\pi}{T} = \sqrt{\Omega^2 - K^2}\end{aligned}\tag{17}$$

$\bar{\Omega}$ is defined to be zero when $K < |\Omega|$; This better illustrates the bifurcation. It is to be noted that this case is too trivial to study the Kuramoto model and naturally we will wish to study the $N=3$ case in the next subsection

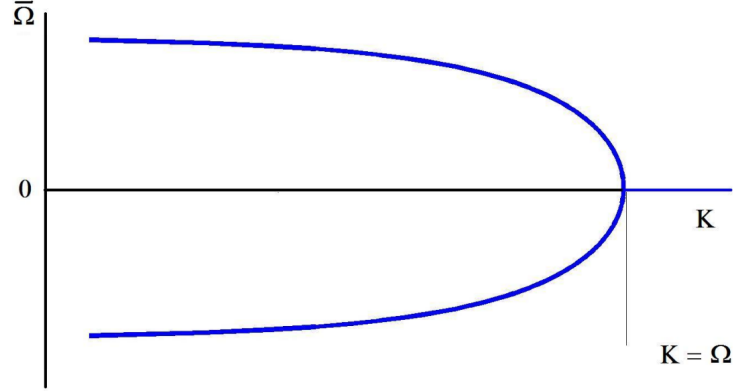


Figure 1:

$\bar{\Omega}$ Vs K It is to be noted that $\lim_{K \rightarrow 0} \bar{\Omega} = \Omega$ since $\bar{\Omega} = \sqrt{\Omega^2 - K^2}$, this also intuitively makes sense, as coupling value gets lower the oscillators will tend to rotate with frequency more closer to their natural frequency.

3.2 3 oscillator system

The analysis of the 3 oscillator system is more involved, The kuramoto model for $N=3$ will be

$$\begin{aligned}\dot{\theta}_1 &= \omega_1 + \frac{K}{3} (\sin(\theta_2 - \theta_1) + \sin(\theta_3 - \theta_1)), \\ \dot{\theta}_2 &= \omega_2 + \frac{K}{3} (\sin(\theta_1 - \theta_2) + \sin(\theta_3 - \theta_2)), \\ \dot{\theta}_3 &= \omega_3 + \frac{K}{3} (\sin(\theta_1 - \theta_3) + \sin(\theta_2 - \theta_3)).\end{aligned}$$

This can be equivalently written as

$$\begin{aligned}\dot{\phi}_1 &= \Omega_1 + \frac{K}{3} (-2 \sin(\phi_1) + \sin(\phi_2 + \phi_1) + \sin(\phi_2)) \\ \dot{\phi}_2 &= \Omega_2 + \frac{K}{3} (-2 \sin(\phi_2) + \sin(\phi_2 + \phi_1) + \sin(\phi_1))\end{aligned} \tag{18}$$

where ,

$$\begin{aligned}\phi_1 &= \theta_2 - \theta_1, & \phi_2 &= \theta_3 - \theta_2, \\ \Omega_1 &= \omega_2 - \omega_1, & \Omega_2 &= \omega_3 - \omega_2.\end{aligned}$$

Additionally,

$$\phi_3 = \theta_1 - \theta_3 = -(\phi_1 + \phi_2).$$

We will restrict ourselves to the special case $\Omega_1 = \Omega_2$ and try to solve the system for the fixed point ($\dot{\phi}_1 = \dot{\phi}_2 = 0$). Our intention of choosing $\Omega_1 = \Omega_2 := \Omega$ proves useful as solving without non-zero constant terms is an easier equation to solve and will also prove helpful in analyzing the flow around these fixed points using the jacobian matrix.

$$\begin{aligned} \dot{\phi}_1 = \dot{\phi}_2 &= 0 \\ \implies -2\sin(\phi_1) + \sin(\phi_2 + \phi_1) + \sin(\phi_2) &= -2\sin(\phi_2) + \sin(\phi_2 + \phi_1) + \sin(\phi_1) \\ \implies \sin(\phi_1) &= \sin(\phi_2) \\ \implies \phi_1 = \pi - \phi_2 \text{ or } \phi_1 &= \phi_2 \end{aligned} \tag{19}$$

- $\phi_1 = \phi_2 = \phi$: In this case both equation in eq(18) are equal and solving for their fixed points results in

$$0 = \frac{3\Omega}{K} - (\sin(\phi) + \sin(2\phi)) \tag{20}$$

for strong coupling $|\Omega| \gg K$:

$$\sin(\phi) + \sin(2\phi) = 0 \tag{21}$$

We observe the points $(\phi_1, \phi_2) = (0, 0), (\frac{2\pi}{3}, \frac{2\pi}{3}), (\pi, \pi), (\frac{4\pi}{3}, \frac{4\pi}{3})$ are stationary points from the fig.2 we observe as K decreases ,first $(\pi, \pi), (\frac{4\pi}{3}, \frac{4\pi}{3})$ coalesce after which $(0, 0), (\frac{2\pi}{3}, \frac{2\pi}{3})$ and coalesce .

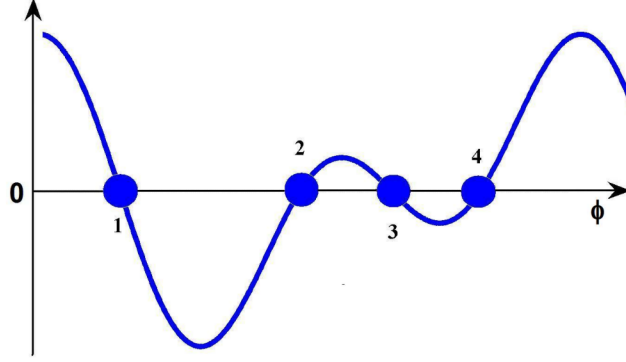


Figure 2:

The above plot represents $\dot{\phi}$ as a function of ϕ for $K \gg \Omega$; for $1 \gg K$ there will be no fixed points due to negligible coupling and as K increases fixed points will be formed in pairs and four stationary points can be observed as in the figure for $K \gg 1$

- $\phi_1 + \phi_2 = \pi$: We observe that this branch adds two new solutions $(\phi_1, \phi_2) = (0, \pi), (\pi, 0)$ these points will coalesce with $(\frac{\pi}{2}, \frac{\pi}{2})$ and eventually coalesces with $(0, 0)$ as K decreases

To analyze the local behavior of these stationary points we calculate the jacobian of the matrix which captures only the linear behavior around the fixed points. The jacobian J for this system can be found by computing the partial derivatives ,

Thus, the Jacobian matrix J for the system is:

$$J = \begin{pmatrix} \frac{K}{3}(-2\cos(\phi_1) - \cos(\phi_2 + \phi_1)) & \frac{K}{3}(\cos(\phi_1) - \cos(\phi_2 + \phi_1)) \\ \frac{K}{3}(\cos(\phi_1) - \cos(\phi_2 + \phi_1)) & \frac{K}{3}(-2\cos(\phi_2) + \cos(\phi_2 + \phi_1)) \end{pmatrix}$$

dropping $\frac{K}{3}$ Jacobian matrix for the system is:

$$J = \begin{pmatrix} -2\cos(\phi_1) - \cos(\phi_2 + \phi_1) & \cos(\phi_1) - \cos(\phi_2 + \phi_1) \\ \cos(\phi_1) - \cos(\phi_2 + \phi_1) & -2\cos(\phi_2) - \cos(\phi_2 + \phi_1) \end{pmatrix}$$

Analyzing the flow along the line $\phi_1 = \phi_2$ the jacobian J simplifies to

$$J = \begin{pmatrix} -2\cos(\phi) - \cos(2\phi) & \cos(\phi) - \cos(2\phi) \\ \cos(\phi) - \cos(2\phi) & -2\cos(\phi) - \cos(2\phi) \end{pmatrix}$$

To find the nature of flow ,we calculate the eigenvalues for the Jacobian matrix . The characteristic equation for the jacobian matrix with eigenvalue λ is

$$(A - \lambda)^2 = B^2 \quad (22)$$

where $A = -2\cos(\phi) - \cos(2\phi)$ and $B = \cos(\phi) - \cos(2\phi)$. The solution

$$\lambda = A \pm |B|$$

can be evaluated at the fixed points and we observe $(0,0)$ is always a stable fixed point and (π, π) is always a saddle point, $(\frac{2\pi}{3}, \frac{2\pi}{3})$ starts as an unstable node but transitions into a saddle point and $(\frac{4\pi}{3}, \frac{4\pi}{3})$ is always an unstable node.

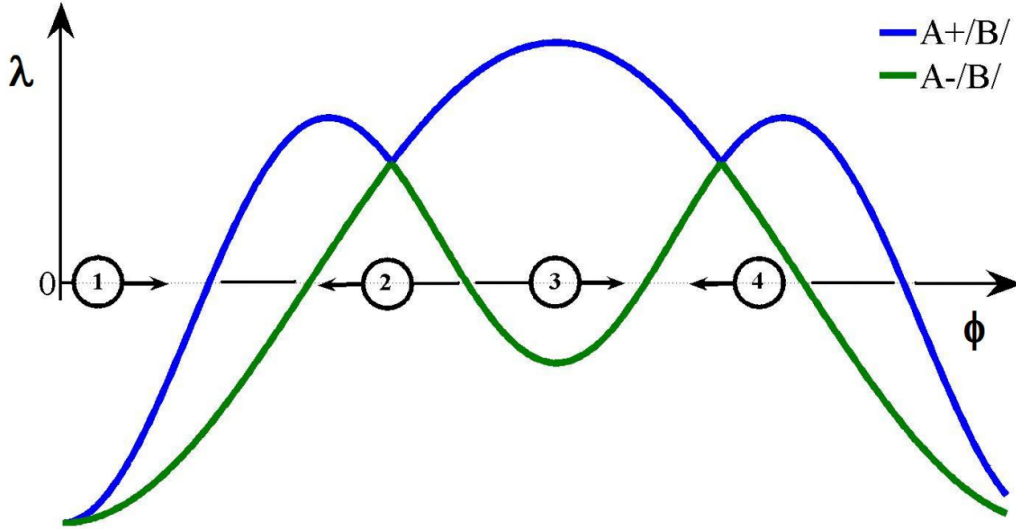


Figure 3:

The above plot represents λ as a function of ϕ for $K \gg \Omega$; here ① = $(0, 0)$, ② = $(\frac{2\pi}{3}, \frac{2\pi}{3})$, ③ = (π, π) , ④ = $(\frac{4\pi}{3}, \frac{4\pi}{3})$. The arrows in the fixed points show the evolution of the fixed points as K decreases from ∞ . It is interesting to observe that the local behavior around the fixed point is not explicitly dependent on Ω rather manifests itself on the Jacobian through the fixed points. Also note that for all ϕ , eigenvectors corresponding to $\lambda(\phi) = A - |B|$ restrict the flow within the line $\phi_1 = \phi_2$.

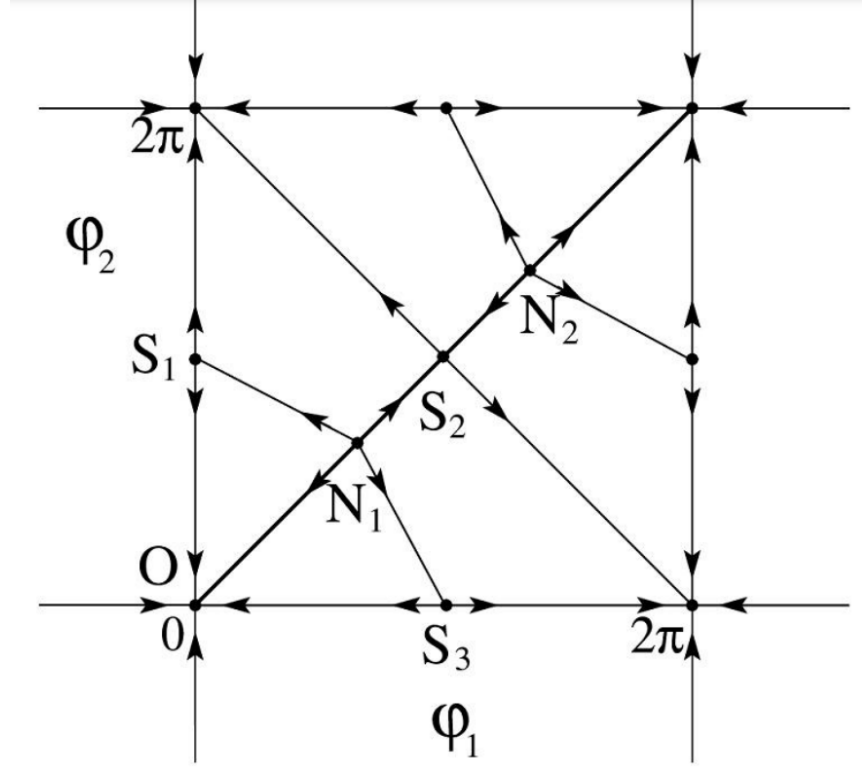


Figure 4:

The stationary points are plotted in the $\phi_1 - \phi_2$ plane where S and N denotes saddle points and Nodes(stable or unstable) .The above plot is done $K \gg 1$

. As K is decreased S_2 and N_2 collapses into a single point followed by the pitchfork bifurcation of S_1 , N_1 and S_3 into a saddle point. At the last the stable node at O and the last unstable node collapses into a semi-stable fixed point

4 Numerical Simulations

Using the Runge-Kutta method for Dynamical systems we can simulate N-oscillator dynamics. Our aim in this section will be to identify the patterns in the behavior of the order parameter as other parameters like N ,K and γ are varied. γ is the parameter from the lorentzian distribution $g(\omega)$. Our primary goal for this section is to relate the results we obtained for the order parameter in section 2 with the numerical results obtained and arrive at some conclusions based on the patterns observed for controlled variations in the parameters.

4.1 R vs t

Plotting order parameter R against time for a random initial condition for a fixed γ value will give an insight on synchronization vs time given no. of oscillators N is sufficiently large. We can plot R against time for different K values to investigate transition from incoherence (random but uniformly chosen initial conditions ensure incoherence) to synchronized state. For $N=100, \gamma = 1$ we get the following plot:

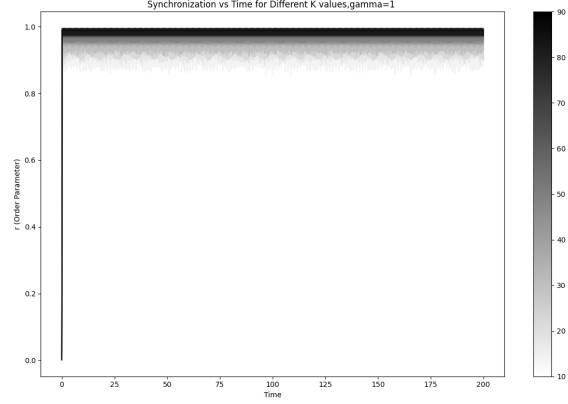


Figure 5: This is the plot of the order parameter against time for K values ranging from 0 to 100

Here, the values of K for the trajectories are indicated by the darkness of the time evolution curves. We observe that for higher values of K , R tends to settle at values closer to 1. But the γ value appears to be a bit small to appreciate the differences in R induced by different K values. Let us see the plot for $\gamma = 10$ and $N = 100$:

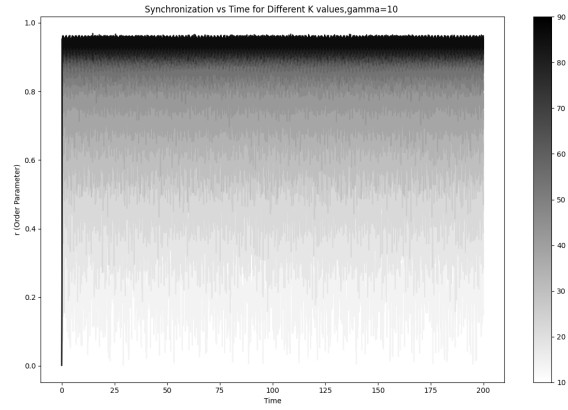
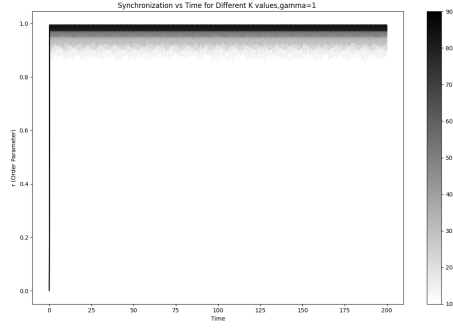
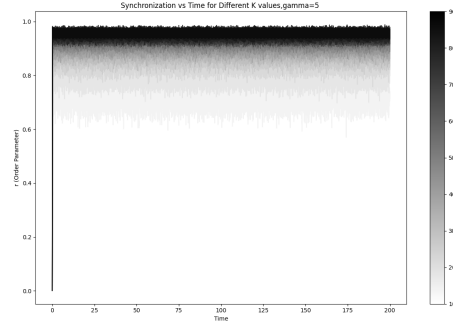


Figure 6: Plot of Order parameter against time for $\gamma = 10$

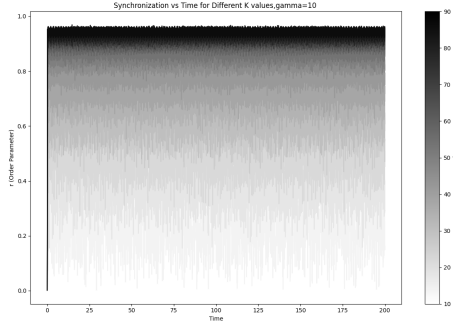
Here we can clearly observe that for the same initial conditions, higher values of K facilitate more synchronization as order parameter R settles at values closer to 1. Apart from verifying the proportionality between R and K we also observe that higher γ values restrict the synchronization and stretches the R values for lower γ , which is evident from the change in γ . To verify this finding, for multiple γ 's, we plot R vs t for various K values.



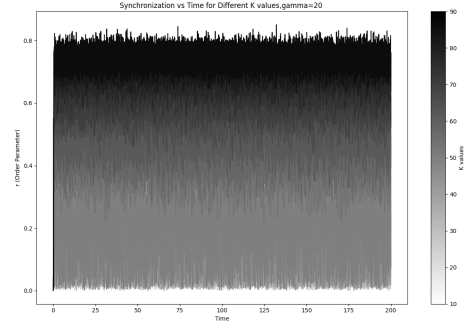
(a) $\gamma = 1$



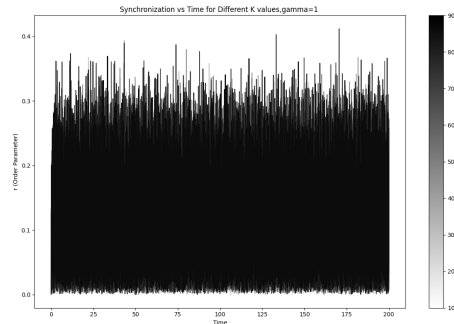
(b) $\gamma = 5$



(c) $\gamma = 10$



(d) $\gamma = 20$



(e) $\gamma = 100$

We observe that for fixed K , as γ is increased the tendency of the system decreases which is evident from the plots. This also aligns well with our expectations. Now instead of investigating time evolution of R for different parameter values we will try to study the average behavior of R which seems natural as we can observe from the plots the R values tend to more or less oscillate around a mean value for majority of the time.

4.2 R vs K

We define \bar{R} as follows:

$$\bar{R} = \frac{1}{n} \sum_{i=1}^n R(i\Delta t) \quad (23)$$

where Δt is the time step, n denotes the no of iterations and t_{ini} is assumed to be zero. The aim of the present study is to investigate \bar{R} as K is varied. Let us look at the plot of R vs K for $\gamma = 5$

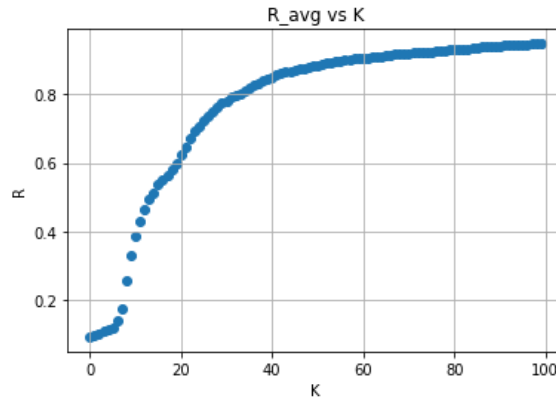
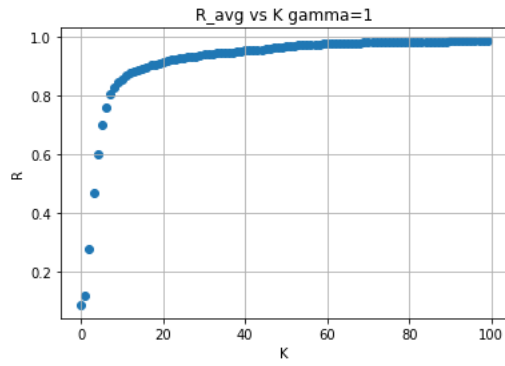


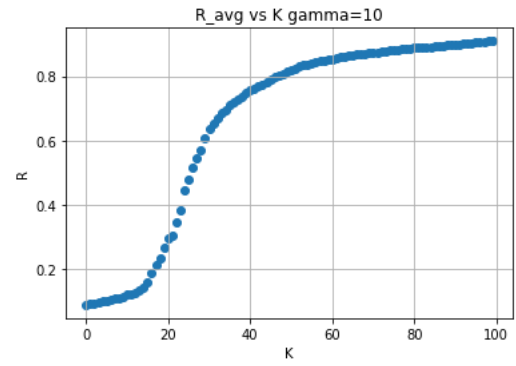
Figure 8: Plot of Order parameter against K for $\gamma = 5$

We observe a steady increase of R , similar to $\sqrt{K - K_c}$ we derived for the Lorentzian distribution. The plot agrees with the analytically obtained result in Section 2.

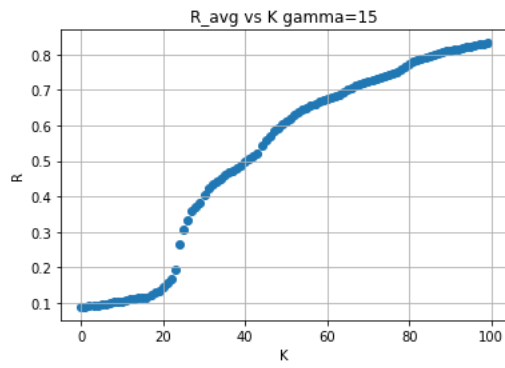
Now we are interested in knowing about the changes we would expect as γ is varied. The plots obtained for various γ are



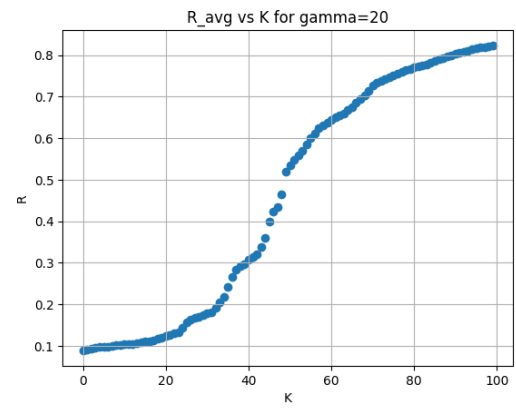
(a) $\gamma = 1$



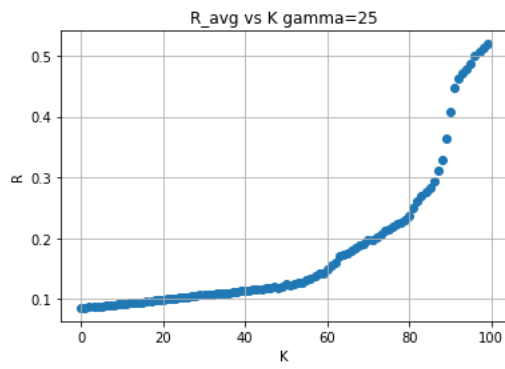
(b) $\gamma = 10$



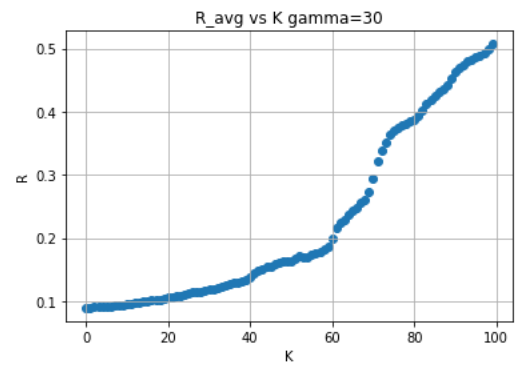
(c) $\gamma = 15$



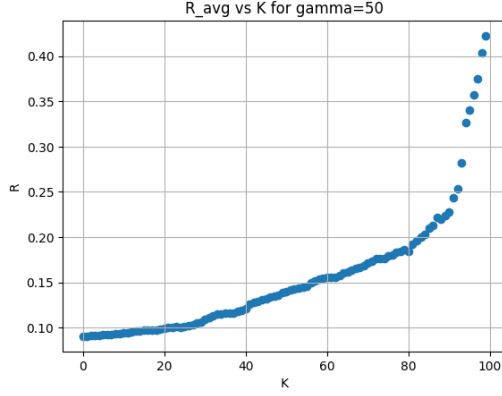
(d) $\gamma = 20$



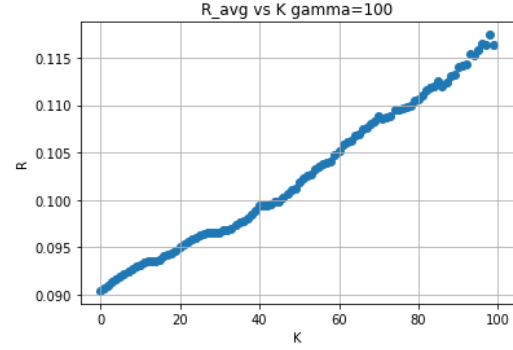
(e) $\gamma = 25$



(f) $\gamma = 30$



(a) $\gamma = 50$



(b) $\gamma = 100$

Figure 10: plots of R vs K for different γ values and $N=100$

From the sets of plots we can conclude that the tendency of the system to synchronize decreases as γ is increased and the critical coupling K_c is also noticed to increase suggestive of the resistance of the system to start synchronizing their phase.

5 Conclusion

The system for Mean field Kuramoto model under the continuum limit were derived and certain branch of solutions were investigated. An approximate equation for r was found for a general natural frequency distribution which will be sufficient to analyze the bifurcation as parameter K is varied. An exact equation for $r(K)$ was derived for the lorentzian distribution of the natural frequency. Bifurcation diagrams for the simple case of $N=2$ and Bifurcation diagram for a special cases of 3 oscillator system were studied extensively and an interesting observation that the local flow around fixed points don't have an explicit Ω dependence was also concluded. At the last, to have an understanding of the time evolution of the system we used Runge-Kutta method and plotted R vs time and R vs K for different distributions and parameters.

References

- [1] J. A. Acebrón, L. L. Bonilla, C. J. Pérez Vicente, F. Ritort, and R. Spigler, “The kuramoto model: A simple paradigm for synchronization phenomena,” *Rev. Mod. Phys.*, vol. 77, pp. 137–185, Apr 2005.
- [2] S. H. Strogatz, “From kuramoto to crawford: exploring the onset of synchronization in populations of coupled oscillators,” *Physica D: Nonlinear Phenomena*, vol. 143, no. 1, pp. 1–20, 2000.